Heliyon 10 (2024) e32356

Contents lists available at ScienceDirect

Heliyon

journal homepage: www.cell.com/heliyon

Research article

Self-doping synthesis of nano-TiO_2 with outstanding antibacterial properties under visible light

Shibin Wu [a,b,c], Jingguang Wang [a,b,c], Zhenze Xie [a,b,c], Chang Du [a,b,c,*]

[a] Department of Biomedical Engineering, School of Materials Science and Engineering, South China University of Technology, Guangzhou, 510641, PR China

[b] National Engineering Research Center for Tissue Restoration and Reconstruction, South China University of Technology, Guangzhou, 510006, PR China

[c] Key Laboratory of Biomedical Materials and Engineering of the Ministry of Education, and Innovation Center for Tissue Restoration and Reconstruction, South China University of Technology, Guangzhou, 510006, PR China

ARTICLE INFO

Keywords:
Self-doping
Nano-TiO_2
Visible light
Antibacterial

ABSTRACT

Nano-TiO_2 photocatalysis technology has attracted wide attention because of its safety, non-toxicity and long-lasting performance. However, traditional nano-TiO_2 has been greatly limited in its application because its wide band gap can only be activated by ultraviolet light ($\lambda < 387$ nm). In this paper, nano-TiO_2 was prepared by self-doping method. The synthesized nano-TiO_2 was a single anatase crystal type with a particle size of 10 nm and uniform size. In addition, nano-TiO_2 has high stability and good dispersion. More importantly, nano-TiO_2 exhibits excellent visible light (400–780 nm) activity due to the decrease of bandgap from 3.20 eV to 1.80 eV (less than 2.0 eV) and the presence of a large number of hydroxyl groups on the surface of the nanoparticles. In the antibacterial test, the antibacterial rate of both E.coli and S.aureus was close to 100 % under the irradiation of household low-power LED lamps, showing excellent antibacterial performance, indicating that the prepared nano-TiO_2 has broad application prospects in the field of bactericidal and bacteriostatic.

1. Introduction

It is indeed true that since the outbreak of COVID-19, there have been an increased focus on anti-viral and anti-bacterial technologies [1]. The development of various antibacterial materials, including polymer antibacterial agents and inorganic antibacterial agents, can be seen as a response to this need. Researchers are working to find more effective and safer ways to protect people from pathogenic bacteria and viruses [2,3].

Polymer antibacterial agents [4,5], such as quaternary amine salt polymeric materials [6,7], have been widely used due to their fast effect and high sterilization rate. However, bacterial resistance has made it difficult for traditional polymer antibacterial agents to persistently harm bacteria. On the other hand, inorganic antibacterial agents, including metal ion type [8,9] and photocatalytic type [10–13], have also gained popularity due to their fast effect and no drug resistance. Metal ion type, such as Ag^+ [14–19], is commonly used; however, there is a hidden danger of secondary harm from metal ions, and the antibacterial performance was weakened with the

* Corresponding author. Department of Biomedical Engineering, School of Materials Science and Engineering, South China University of Technology, Guangzhou, 510641, PR China.

E-mail address: duchang@scut.edu.cn (C. Du).

https://doi.org/10.1016/j.heliyon.2024.e32356
Received 6 February 2024; Received in revised form 17 April 2024; Accepted 3 June 2024
Available online 13 June 2024

release of metal ions. Photocatalytic antibacterial agents, such as nano-TiO_2, are known for their stable and long-lasting antibacterial performance.

In recent years, nano-TiO_2 has been broadly applied in the antibacterial field due to its photocatalytic activity [20–23]. Rahmah [24] prepared TiO_2/graphene nanostructures by combining hydrothermal method with Nd-YAG laser, the sample colloids had a negative electrical charge on their surface, with a zeta potential of around (−16.7) mV. The antibacterial tests showed that TiO_2/graphene nanostructure had a good inhibitory effect on Staphylococcus aureus and Escherichia coli bacteria with inhibition zones of 36 and 29 mm, respectively. Awan et al. [25] synthesized pure TiO_2 and $MnTiO_2$ nanoparticles using the defect-oriented hydrothermal method, $MnTiO_2$-NPs showed significantly higher photocatalytic activity than pure TiO_2.The antibacterial activity was also tested against E. coli and S. aureus, $MnTiO_2$-NPs shows superior antibacterial efficacy than pure TiO_2. Rilda et al. [26] prepared ZnO–TiO_2 nanorods with route precipitation and sintering at 600 °C, then ZnO–TiO_2 was coated on cotton cloth using a dip-spin method. The improvement of Pseudomonas aeruginosa antibacterial properties in the textiles with coating had an inhibition zone of 20.5–25.0 mm and 16.2 mm without the coating, which could be successfully applied to improve the antibacterial properties of textiles.

Nevertheless, there are two main problems limiting the further development of this technology. First, most nano-TiO_2 preparation technologies result in nano-TiO_2 powders, such as sol-gel method [27,28], precipitation method [29], hydrothermal method [30,31], etc. However, nano-TiO_2 powders are difficult to be dispersed and used in late applications, especially in large-scale industrial production applications. In addition, nano-TiO_2 powder is easy to agglomerate during storage and lose the characteristics of nanomaterials. Second, in the existing nano-TiO_2 doping modification [32,33] and self-doping methods [34,35], due to the difficulty in reducing the band gap below 2.0 eV, its visible light activity is not high, so that some papers, when describing its application in visible light, can only use hundreds of watts of high-power lamp irradiation to achieve certain effect [36–39]. So the practical value is too low.

Herein, we prepared nano-TiO_2 by self-doping method, as shown in Scheme 1. This method not only solved problems related to practical application and poor long-term storage stability, but also provided a good visible light activity and excellent antibacterial properties under the irradiation of household low-power LED lamps.

2. Experimental section

2.1. Materials

Titanium (IV) oxysulfate-sulfuric acid hydrate (purity 93 %) and polyethylene glycol 200 (PEG-200, AR) were purchased from Macklin (Shanghai, China). Barium hydroxide ($Ba(OH)_2$, AR), Benzoquinone were purchased from Aladdin (Shanghai, China). Nitric acid (HNO_3, AR) was purchased from Tianjin Damao Chemical Reagent Factory. Commercially nano-TiO_2 (VK-TA15) was purchased from Xuancheng Jingrui New Material Co., LTD. Methylene blue (MB, AR) was supplied by Tianjin Tianxin Fine Chemical Development Center. Red ink (M&G brand) was purchased from Shanghai M&G Stationery Co., LTD. Isopropyl alcohol (AR) was purchased from Ruishengxiang. EDTA disodium salt was purchased from guangzhou chemical reagent factory. Silver nitrate was purchased from sinopharm group chemical reagent Co., LTD. All of materials without further processing.

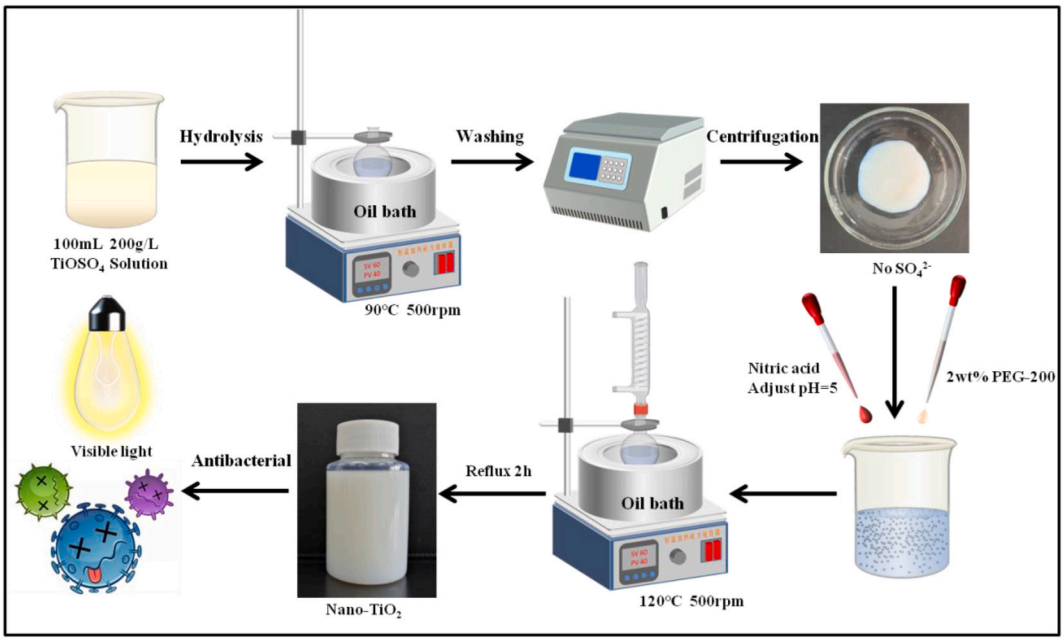

Scheme 1. The nano-TiO_2 with antibacterial activity under visible light was prepared by self-doping method.

2.2. Preparation of nano-TiO_2 and characterization

Nano-TiO_2 was prepared in two steps by self-doping method. In the first step, a titanium oxide sulfate solution (20 mL, 200 g/L) was added into 20 mL deionized water at 90 °C and stirred at 500 rpm until a light blue material appeared. Then, another titanium oxide sulfate solution (80 mL, 200 g/L) was quickly poured in and stirred for 30 min. Finally, the resulting solution was washed with water to remove sulfate ions [40], and tested for residual sulfate ions with barium hydroxide. Then pure titanium hydroxide was separated by centrifugation at 3000 rpm. For the second step, the above centrifuged titanium hydroxide was dispersed into 100 mL deionized water and adjusted to pH = 5 with nitric acid, and 2 wt% of PEG-200 was added as dispersant. Then, the solution was placed in an oil bath at 120 °C for condensation reflux 2 h for crystallization. Finally, nano-TiO_2 solution was obtained (Fig. 1a).

The morphology of nano-TiO_2 was obtained by field emission scanning electron microscope (SEM, Zeiss Gemini 300), and transmission electron microscope (TEM, Talos L120C). X-ray diffraction (XRD, D8 Advance) measurements were performed to verify the crystal structure of nano-TiO_2 at a scanning rate of $1^{\circ}min^{-1}$ in the 2θ range from 20° to 80°, with graphite monochromatized Cu Kα radiation. Moreover, Raman spectrometer (RS, Renishaw invia) was used to study the crystal type.

2.3. The photocatalytic activity of nano-TiO_2 and its mechanism

The photocatalytic activity test of nano-TiO_2 involved three parameters: visible light catalytic activity, the durability of its performance and the stability of nano-TiO_2 solution. Firstly, for testing visible light catalytic activity, methylene blue (MB) was used as a simulated pollutant. A 0.1 wt% solution of nano-TiO_2 with MB added (final concentration of 10 ppm) was kept under visible light irradiation (15W, LED lamp, the wavelength is 450–460 nm) for around 25 h. The control group was a 2 mL deionized water solution with MB added (final concentration of 10 ppm) that underwent the same conditions. Both reactions were recorded by taking pictures, and the absorbance change of MB was monitored using UV–vis spectrophotometer (TU-1901) at a wavelength of 650 nm.

Secondly, red ink was used to evaluate the durable stability of photocatalytic activity. To be specific, one drop of red ink was mixed with 100 mL of 1 wt% nano-TiO_2 solution and stirred evenly. This mixed solution was then placed under household light (light intensity of 1.10 W/m^2) for 20 h and then the color of solution was observed. This process was repeated 18 times in sequence while maintaining a volume of 100 mL of solution. These tests can accurately evaluate the visible light activity and stability of the prepared nano-TiO_2 under household low-power LED lamps.

The X-ray photoelectron spectra (XPS, Escalab Xi+), Fourier Transform Infrared Spectroscopy (FT-IR, iS50), UV–vis spectrophotometer (UV–vis, TU-1901) and fluorescence spectroscopy (PL, F-7000) allowed the study of the mechanism of visible light activity.

The degradation mechanism of dyes through photocatalysis is further examined using scavenger tests. Traditionally, electrons (e^-), holes (h^+), super hydroxyl radicals (·OH), and superoxide radicals ($\cdot O_2^-$) are considered as the active species responsible for the

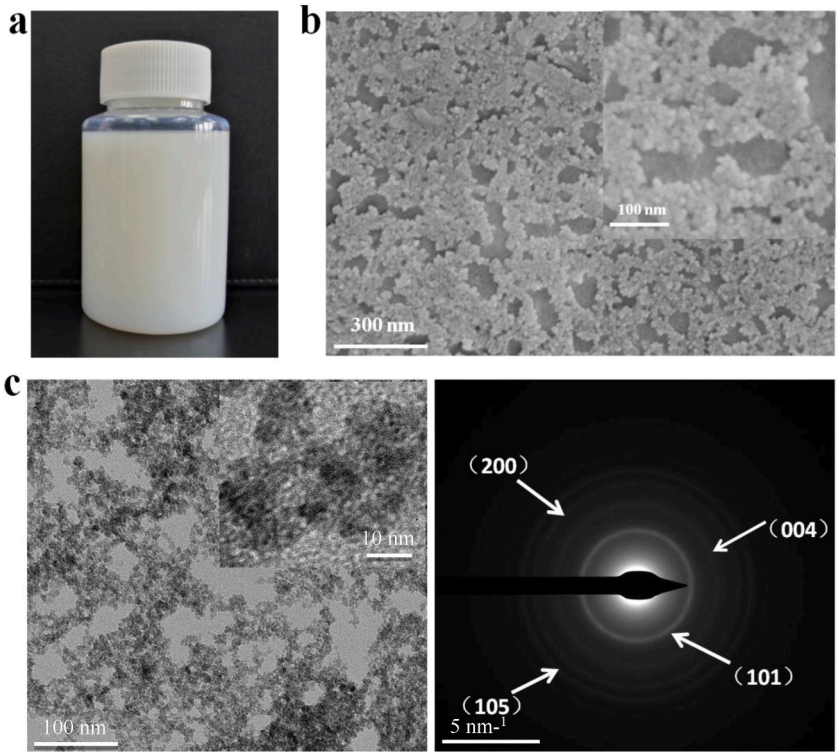

Fig. 1. Characterization of nano-TiO_2: (a) Digital photograph (b) SEM image; (c) TEM and SAED patterns.

photodegradation of organic dyes. In order to distinguish the role of each radical in the degradation of MB and nano-TiO_2, scavengers such as silver nitrate ($AgNO_3$), EDTA disodium salt (EDTA-2Na), isopropanol (IPA), and benzoquinone (BQ) are individually added to solutions as sacrificial agents, respectively [41]. Subsequently, photocatalytic experiments are repeated under visible light. Scavenger experiment and cyclic experiment parameters: The light source was a LED lamp (15 W), the concentration of MB was 1 ppm, the solvent dosage was 15 mM, the concentration of nano-TiO_2 was 0.5 wt%, and the absorbance was tested at a wavelength of 650 nm.

2.4. Antibacterial evaluation

The antibacterial activity of nano-TiO_2 was analyzed using two methods in this study: the inhibition zone method and the colony counting method. The antibacterial activity was qualitatively analyzed by the size of the inhibition circle, and the antibacterial rate was quantitatively analyzed by the number of bacterial residues after the antibacterial experiment.

In the analysis of bacteriostatic zone, two methods were used, which were compared with commercially nano-TiO_2 powder and different conditions of oneself. In comparison with the commercially nano-TiO_2 powder, 200 μL (10^7 CFU mL^{-1}) S. aureus was uniformly coated on the nutrient agar plate, and then the nano-TiO_2 liquid with same solid content of 50 μL was dropped onto the same agar plate. One group was irradiated under 365 nm ultraviolet lamp for 2 h and put into 37 °C constant temperature and humidity incubator; the other group was put into 37 °C constant temperature and humidity incubator and continuously exposed to visible light (LED lamp of 2.5 W, light intensity of 3.42 W/m^2), and the antibacterial zone effect was checked after 24 h. In the comparison of different conditions, 200 μL bacterial solution (S. aureus or E. coli, 10^9 CFU mL^{-1}) was evenly coated on the nutrient agar plate, and then 50 μL nano-TiO_2 was dropped on the agar plate, and one group was put into a 37 °C constant temperature and humidity incubator and continuously exposed to visible light (LED lamp of 2.5 W, light intensity of 3.42 W/m^2), and the other group was also put into a constant temperature and humidity incubator at 37 °C but was dark treated with tin foil wrap, and the effect of antibacterial circle was checked after 24 h.

The antibacterial effect was quantified by the colony counting method, which allowed the antibacterial efficacy assessment using the colony-forming units method (CFU). The nano-TiO_2 liquid (10 mg/mL) was dropped into the bacterial solution (E. coli or S. aureus, at a concentration of 10^4 CFU mL^{-1}), then placed on a shaker at 100 rpm for co-culture under household light (light intensity of 1.10 W/m^2) or not for 3 h. Then the 200 μL co-cultured bacterial solution was evenly coated on the nutrient agar plate and cultured at 37 °C for 24 h, the antibacterial rate was calculated by the number of colonies.

3. Results and discussion

3.1. The characterization of nano-TiO_2

We prepared nano-TiO_2 which could remain stable under static conditions and no precipitation was produced (Fig. 1a). In order to study the size and distribution of nano-TiO_2 particles, SEM and TEM were performed on them. The nano-TiO_2 uniformly dispersed with a mean size of 10 nm without large reunion (Fig. 1b and c), which provided basic condition for the long-term stable existence of nano-TiO_2 solution. Furthermore, nano-TiO_2 colloid solution exhibited the Tyndall effect (Fig. S1), this also explained.

from another perspective why nano-TiO_2 particles could stably exist in water. A slight aggregation detected by DLS and the average particle size was 68 nm (Fig. S2). The strong electrostatic forces between the nanoparticles enable them to remain suspended in the solution. The average potential of nano-TiO_2 particles was +35.8 mV (Fig. S2), indicated that the nano-TiO_2 particles prepared in this study had a positively charged surface with a large charge magnitude, which was the main reason for the long-term stability of nano-TiO_2 particles.

The crystal form of nano-TiO_2 was determined by SAED, XRD and Raman spectra. The SAED pattern (Fig. 1c) clearly revealed the presence of (101), (004), (200), and (105) anatase TiO_2 concentric diffraction rings, which confirmed that nano-TiO_2 was anatase crystal form and polycrystalline form [42]. XRD peaks (Fig. 2a) were observed at 2θ values approximately 25.3, 37.9, 48.0, 54.0, 55.1, 62.7, 68.9, 70.3, and 75.2° corresponding to the anatase phase (101), (004), (200), (105), (211), (204), (116), (220) and (215) of their crystalline structure of anatase form (JCPDS, No:21–1272). The Raman spectra showed in Fig. 2b, the E_g peak was mainly caused by

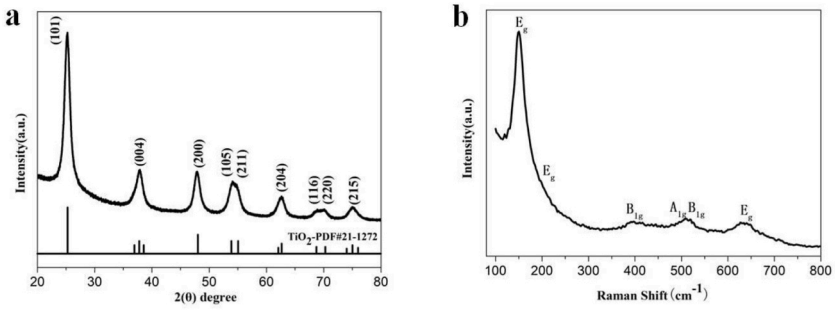

Fig. 2. XRD patterns (a) and Raman spectra (b) of nano-TiO_2.

symmetric stretching vibration of O–Ti–O in TiO_2, the B_{1g} peak was caused by symmetric bending vibration of O–Ti–O, and the A_{1g} peak was caused by antisymmetric bending vibration of O–Ti–O [43]. Importantly, the peaks appeared at 144, 394, 515, and 640 cm^{-1} were the typical peaks of anatase TiO_2 phase [44].

Therefore, these results proved that the nano-TiO_2 particles prepared in this study were single anatase crystal type. However, the crystallinity of nano-TiO_2 was not high, accompanied by a small amount of amorphous, these defects provided material basis for self-doping.

3.2. The photocatalytic activity of nano-TiO_2 and its mechanism

We compared the spectral absorption and the band gap between the nano-TiO_2 liquid prepared in this work (experimental group) and the commercially purchased nano-TiO_2 powder (control group). The nano-TiO_2 liquid prepared in this work had great absorption in the visible light region (400–780 nm) rather than commercially available nano-TiO_2 according to the UV–vis spectroscopy (Fig. 3a). Moreover, the Eg = 1.80 eV of the nano-TiO_2 prepared in this work was much lower than that of the commercially available product (Eg = 3.20 eV) by calculating the band gap of two products (Fig. 3b). Both the spectral absorption range and the band gap confirmed that the nano-TiO_2 prepared in this work had good absorption in the visible light region, and the band gap was greatly narrowed, which strongly proved the internal basis for its excellent visible light activity [45].

The photocatalytic activity of the nano-TiO_2 prepared in this work and the commercially purchased nano-TiO_2 powder was reflected by the PL analysis and MB degradation experiment. The higher the fluorescence spectral peak, the larger the electron-hole pair recombination, resulting in lower photocatalytic activity. As shown in Fig. 3c, the peak of nano-TiO_2 prepared in this work was lower than that of the commercially available, indicating that its photogenerated electron-hole pair was less recombination, the more hydroxyl radical produce by nano-TiO_2, the higher photocatalytic activity is. So the photocatalytic activity was better. As shown in Fig. 3d, the experimental group (red line) was significantly lower than the control group (black line), represented that MB was degraded more by nano-TiO_2 prepared in this study (percentage of decomposition was 81.4 %), indicated that the photocatalytic activity was better.

Furthermore, in order to fully confirm the visible light activity of nano-TiO_2 and subsequent long-term antibacterial applications,

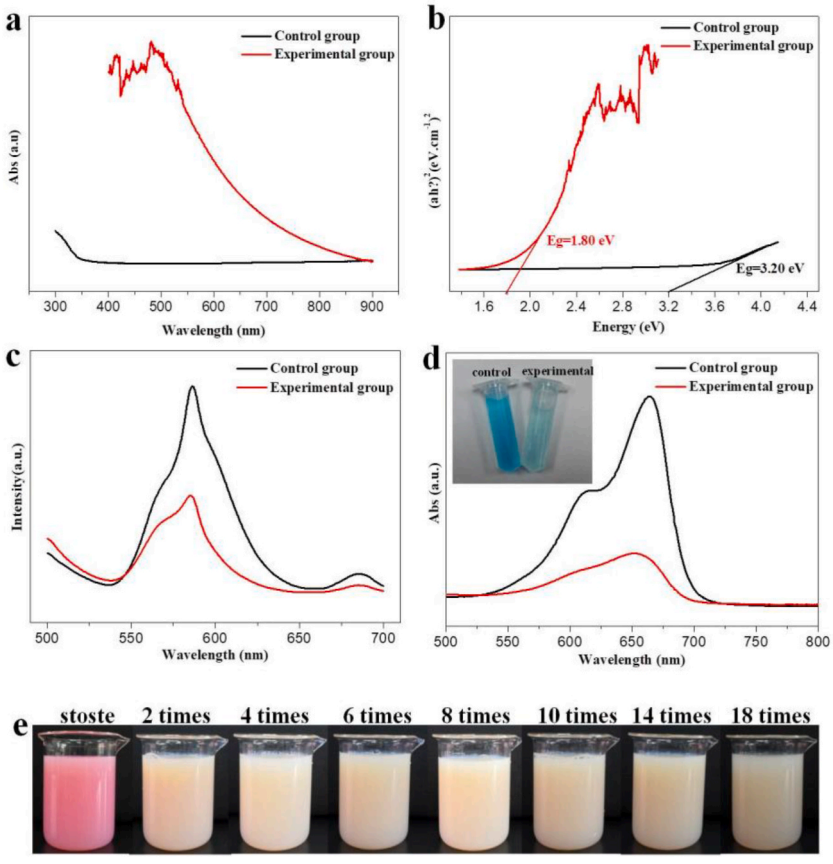

Fig. 3. UV–vis spectra(a-b) and PL spectra(c) of nano-TiO_2, Absorbance spectra of photodegradation of MB(d) with nano-TiO_2 under the irradiation of visible light, Digital photograph of degradation continuously red ink(e) with nano-TiO_2 under the irradiation of visible light. (For interpretation of the references to color in this figure legend, the reader is referred to the Web version of this article.)

the red ink was used as a simulated pollutant to test its durability and stability of visible light activity. As shown in Fig. 3e, the prepared nano-TiO_2 could continuously degrade red ink under visible light conditions for many times and remained stable without polymerization, indicating that nano-TiO_2 had good durability and stability of visible light activity, which provided the possibility for the application of long-term antibacterial [46].

As known, electrons (e^-), holes (h^+), hydroxyl radicals (•OH), and superoxide radicals ($\bullet O_2^-$) are considered as potential active species involved in the photocatalytic degradation of organic pollutants [41]. In order to identify the active species during the photocatalytic reaction, scavengers such as $AgNO_3$, EDTA-2Na, IPA, and BQ were introduced into the MB solution. As shown in Fig. 4a, the addition of $AgNO_3$ and EDTA-2Na had a minimal impact on the photocatalytic activity, indicating that e^- and h^+ may not be the primary active species in the photocatalytic process. The degradation efficiency decreased upon the addition of IPA, confirming the role of •OH as an active species. Moreover, the photocatalytic performance was significantly hindered following the introduction of BQ, underscoring the crucial involvement of $\bullet O_2^-$ in the photocatalytic degradation process. Moreover, in order to further investigate its stability, cycling experiments were conducted. As shown in Fig. 4b, after four cycles of operation, the degradation rate of MB showed little decline. The results indicate that nano-TiO_2 exhibits good cycling stability.

To study the intrinsic cause of its photocatalytic activity, the element composition and the valence states of the nano-TiO_2 were evaluated via XPS. The nano-TiO_2 contained Ti, O, C and S elements, and the contents of which were 10.41 %, 74.14 %, 14.65 % and 0.78 % respectively (Fig. 5a). Among them, the element S and C came from the residue of SO_4^{2-} in titanium oxysulfate and PEG-200 in the raw material for the preparation of nano-TiO_2, respectively. Fig. 5b showed that the peaks in the TiO_2 were at the binding energies 458.5 eV (Ti2p3/2) and 464.2 eV (Ti2p1/2) respectively. Compared with the Ti2p3/2 peak of traditional nano-TiO_2, the Ti2p3/2 peak of nano-TiO_2 prepared in this paper had a significant shift, decreasing from 458.7 eV to 485.5 eV, which may be the reason for the existence of Ti^{3+}. Since Ti^{3+} species had a lower 2p3/2 binding energy than Ti^{4+}, so the presence of Ti^{3+} caused the Ti2p3/2 peak to move towards a lower binding energy [34]. It could be seen from Fig. 5c that three characteristic peaks could be fitted at 529.8 eV, 531.9 eV and 533.3 eV, they correspond to Ti–*O*–Ti, Ti–OH and C–O [47], respectively. Where the characteristic peak at 530 eV was the characteristic peak of lattice oxygen, and the characteristic peak at 532 eV could be attributed to the oxygen in hydroxy-OH and O_2 adsorbed on the surface. The characteristic peak at 533 eV was the oxygen in the surface adsorbed species [48]. From the above analysis, it could be seen that Ti^{3+} self-doped nano-TiO_2 ($w(Ti^{3+}) = 40.1$ %) and the abundant hydroxyl groups on the surface of nano-particles provided the high visible light activity of nano-TiO_2 [49].

In order to explore the relation between photocatalytic activity of nano-TiO_2 and its functional groups, Fourier transform infrared spectroscopy (FT-IR) was performed. From the spectrum (Fig. 5d), it could be seen that there were four obvious peaks of nano-TiO_2, which were 1096 cm^{-1}, 1688 cm^{-1}, 2871 cm^{-1} and 3154 cm^{-1}. The peak at 1096 cm^{-1} was related to the stretching vibrations of Ti–OH molecule [27]. C–H stretching vibration peak corresponding to 2871 cm^{-1} [50]. Finally, the peak at 1688 cm^{-1} and 3154 cm^{-1} was related to the stretching vibrations of the corresponding OH hydroxyl [38,51]. In a word, a large number of –OH hydroxyl groups on the surface of nano-TiO_2 prepared in this study provided favorable conditions for the photocatalytic reaction, which also verified the internal mechanism of high activity of nano-TiO_2 from another dimension [52].

The photocatalytic mechanism can be explained as follows. When nano-TiO_2 is exposed to visible light, electrons in the valence band are excited to the conduction band, generating electron-hole pairs. These electrons react with the surface-adsorbed oxygen to form superoxide radicals $\cdot O_2^-$. Simultaneously, the holes combine with water molecules to produce hydroxyl radicals (·OH). These by-products combine with organic compounds to generate non-toxic carbon dioxide and water as the final products. Photocatalytic mechanism has been depicted in Fig. 6(see Fig. 7).

3.3. Antibacterial analysis of nano-TiO_2

In this study, the antibacterial activity of nano-TiO_2 was comprehensively evaluated by qualitative analysis of the bacteriostatic circle method and quantitative analysis of the colony counting method.

We dropped the solution of the commercially purchased nano-TiO_2 (control) and the nano-TiO_2 prepared in this work (experimental) with the same concentration and pH on the nutrient agar plate coated by the S. aureus and then irradiated under 365 nm

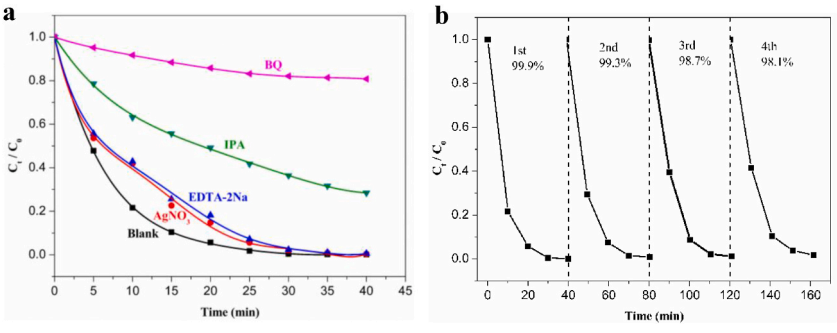

Fig. 4. (a) The photocatalytic degradations of 0.5 wt% nano-TiO_2 with different scavengers; (b) Recycled runs of the degradation under visible light irradiation.

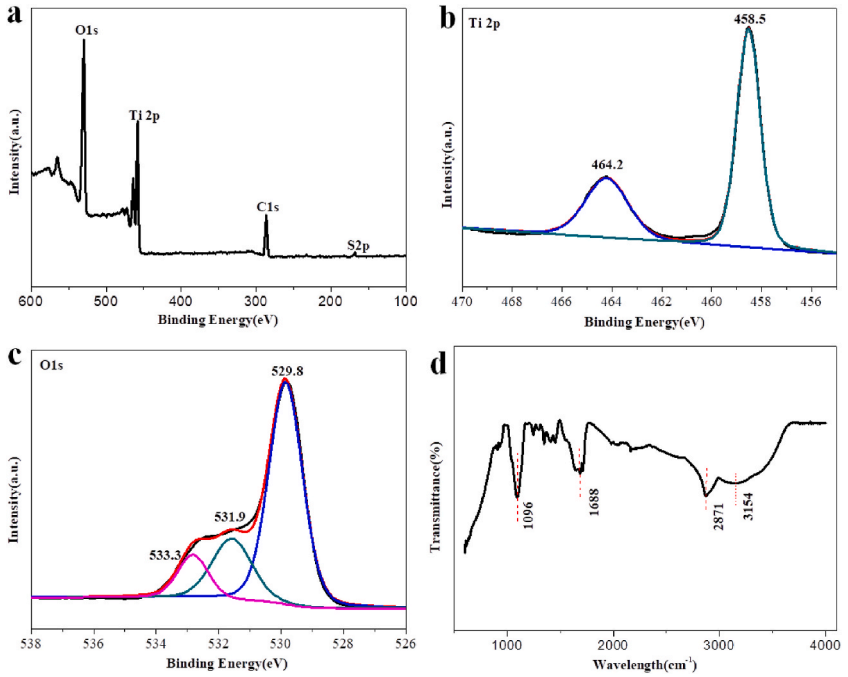

Fig. 5. XPS spectra (a–c) and FT-IR spectra (d) of nano-TiO_2.

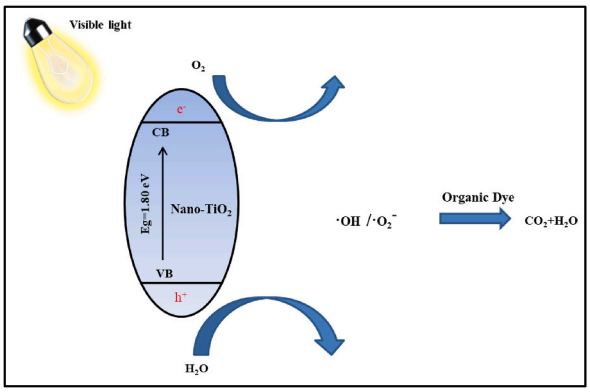

Fig. 6. Photocatalytic mechanism of nano-TiO_2.

ultraviolet or visible light. Both kinds of nano-TiO_2 show antibacterial zone under ultraviolet lamp (Fig.7a), while only the region of nano-TiO_2 prepared in this work showed bacteriostatic zone under LED illumination (Fig.7b), verified that nano-TiO_2 had better antibacterial activity compared with commercial nano-TiO_2 under visible light.

Furthermore, the inhibitory effect of nano-TiO_2 prepared in this work on S. aureus and E. coli under the presence or absence of visible light was also explored (Fig. 8). There was no bacteriostatic circle whatever S. aureus or E. coli group under.

darkness, nevertheless, the pronounced bacteriostatic circle appeared in both groups under irradiation of visible light (Fig. 8a_1-a_2/b_1-b_2). Moreover, the colony-forming unit method was used to quantitatively evaluate the antibacterial effect. Both the groups cocultured with nano-TiO_2 under darkness group (Fig. 8a_3/b_3) and without nano-TiO_2 under irradiation of visible light (Fig. 8a_4/b_4) grew a large number of colonies. However, the group cocultured with nano-TiO_2 under irradiation of visible light (Fig. 8 a_5/b_5) had no bacterial colonies and exhibited an excellent antibacterial effect (the antibacterial rate was almost 100 %). It proved that the nano-TiO_2 prepared in this study had excellent visible light activity and broad-spectrum antimicrobial property [46].

4. Conclusion

In this study, the nano-TiO_2 with excellent visible light activity and broad-spectrum antimicrobial property was synthesized by self-doping method using inorganic titanium source titanium oxide sulfate. The particle size of the prepared nano-TiO_2 was found to be

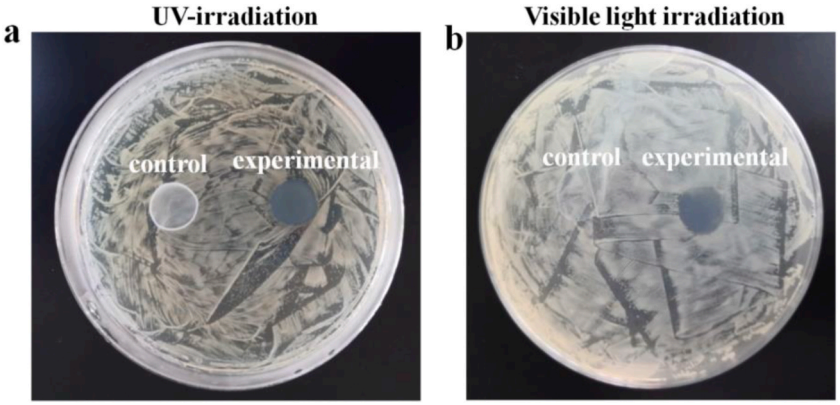

Fig. 7. Antibacterial activity of different nano-TiO_2 (control: commercially nano-TiO_2; experimental: nano-TiO_2 prepared in this study).

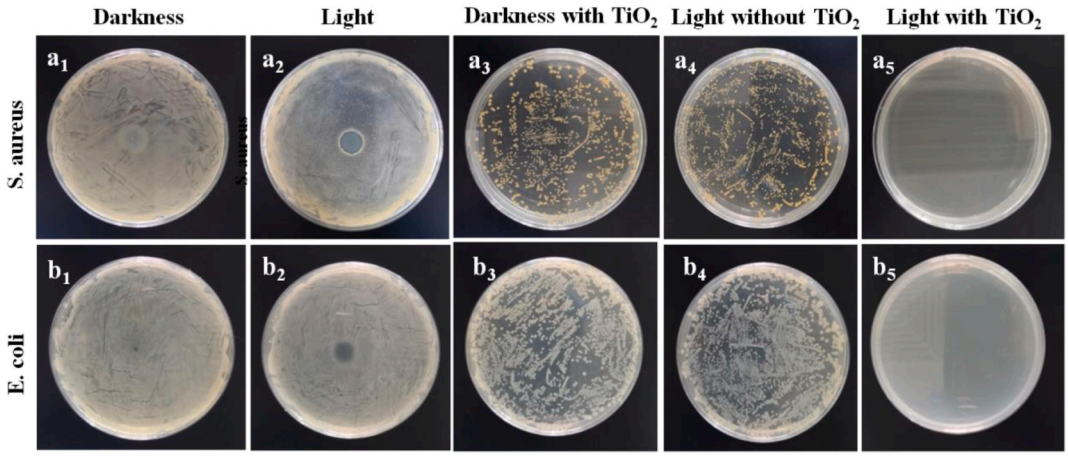

Fig. 8. Antibacterial activity of nano-TiO_2 under different conditions against E. coli and S. aureus by the inhibition zone method(a_1-a_2/b_1-b_2) and the colony counting method(a_3-a_5/b_3-b_5) (a_1/b_1: darkness; a_2/b_2: light; a_3/b_3: darkness with TiO_2; a_4/b_4: light without TiO_2; a_5/b_5: light with TiO_2).

uniform at about 10 nm, and the particles were spherical and uniformly dispersed without large agglomeration. The crystal form of the nano-TiO_2 was single anatase. Compared with commercially available nano-TiO_2 products, Ti^{3+} self-doped nano-TiO_2 had a wider light absorption range, a narrower band gap (Eg = 1.80 eV) and a lower photogenerated electron-hole pair recombination rate. The prepared nano-TiO_2 particles could continuously degrade red ink under visible light condition for many times and remain stable, showing very good performance durability and stability. The antibacterial results showed that the nano-TiO_2 had excellent broad-spectrum antibacterial properties under the irradiation of household low-power LED lamps, and the antibacterial rate was almost 100 %. Therefore, the nano-TiO_2 prepared in this study has a high market application prospect in the field of bactericidal and bacteriostatic.

Data availability

Data will be made available on request.

CRediT authorship contribution statement

Shibin Wu: Writing – review & editing, Writing – original draft, Investigation, Formal analysis, Data curation, Conceptualization. **Jingguang Wang:** Writing – review & editing, Writing – original draft, Methodology, Investigation, Formal analysis, Data curation. **Zhenze Xie:** Visualization, Validation, Formal analysis. **Chang Du:** Writing – review & editing, Supervision, Resources, Project administration, Investigation, Funding acquisition, Formal analysis, Conceptualization.

Declaration of competing interest

There are no conflicts to declare.

Acknowledgments

Shibin Wu and Jingguang Wang contributed equally to this work. This work was supported by theFoundation of National Key Research and Development Program of China (2023YFB3809900). The authors would like to thank the help of Ken Liu (from South China University of Technology) in preparation and Tianyu Wei (from South China University of Technology) for his efforts in the TEM analysis.

Appendix A. Supplementary data

Supplementary data to this article can be found online at https://doi.org/10.1016/j.heliyon.2024.e32356.

References

[1] C. Weiss, M. Carriere, L. Fusco, I. Capua, J.A. Regla-Nava, M. Pasquali, J.A. Scott, F. Vitale, M.A. Unal, C. Mattevi, D. Bedognetti, A. Merkoci, E. Tasciotti, A. Yilmazer, Y. Gogotsi, F. Stellacci, L.G. Delogu, Toward Nanotechnology-Enabled approaches against the COVID-19 pandemic, ACS Nano 14 (2020) 6383–6406, https://doi.org/10.1021/acsnano.0c03697.

[2] J. Kim, J. Jang, Inactivation of airborne viruses using vacuum ultraviolet photocatalysis for a flow-through indoor air purifier with short irradiation time, Aerosol Sci. Technol. 52 (2018) 557–566, https://doi.org/10.1080/02786826.2018.1431386.

[3] Z.Q. Xu, Y. Wu, F. X Shen, Q. Chen, M.M. Tan, M.S. Yao, Bioaerosol science, technology, and engineering: past, present, and future, Aerosol Sci. Technol. 45 (2011) 1337–1349, https://doi.org/10.1080/02786826.2011.593591.

[4] L.J. Sun, S.S. Yang, X.R. Qian, X.H. An, High-efficacy and long term antibacterial cellulose material: anchored guanidine polymer via double “click chemistry”, Cellulose 27 (2020) 8799–8812, https://doi.org/10.1007/s10570-020-03374-5.

[5] T.T. Zhou, R. Hu, L.R. Wang, Y.P. Qiu, G.Q. Zhang, Q.Y. Deng, H.Y. Zhang, P.G. Yin, B. Situ, C.L. Zhan, A.J. Qin, B.Z. Tang, An AIE-active conjugated polymer with high ROS-generation ability and biocompatibility for efficient photodynamic therapy of bacterial infections, Angew. Chem. Int. Ed. 59 (2020) 9952–9956, https://doi.org/10.1002/anie.201916704.

[6] Y. Han, Z.C. Zhou, L. Zhu, Y.Y. Wei, W.Q. Feng, L. Xu, Y. Liu, Z.J. Lin, X.Y. Shuai, Z.J. Zhang, H. Chen, The impact and mechanism of quaternary ammonium compounds on the transmission of antibiotic resistance genes, Environ. Sci. Pollut. Res. 26 (2019) 28352–28360, https://doi.org/10.1007/s11356-019-05673-2.

[7] P.I. Hora, S.G. Pati, P.J. McNamara, W.A. Arnold, Increased use of quaternary ammonium compounds during the SARS-CoV-2 pandemic and beyond: consideration of environmental implications, Environ. Sci. Technol. Lett. 7 (2020) 622–631, https://doi.org/10.1021/acs.estlett.0c00437.

[8] S. Stankic, S. Suman, F. Haque, J. Vidic, Pure and multi metal oxide nanoparticles: synthesis, antibacterial and cytotoxic properties, J. Nanobiotechnol. 14 (2016) 73, https://doi.org/10.1186/s12951-016-0225-6.

[9] G. Wyszogrodzka, B. Marszalek, B. Gil, P. Dorozynski, Metal-organic frameworks: mechanisms of antibacterial action and potential applications, Drug Discov. Today 21 (2016) 1009–1018, https://doi.org/10.1016/j.drudis.2016.04.009.

[10] N. Nithya, G. Bhoopathi, G. Magesh, C.D.N. Kumar, Neodymium doped TiO_2 nanoparticles by sol-gel method for antibacterial and photocatalytic activity, Mater. Sci. Semicond. Process. 83 (2018) 70–82. https://dor.org/10.1016/j.mssp.2018.04.011.

[11] E. D Lucas-Gil, P. Leret, M. Monte-Serrano, J.J. Reinosa, E. Enriquez, A.D. Campo, M. Canete, J. Menendez, J.F. Fernandez, F. Rubio-Marcos, ZnO nanoporous spheres with broad-spectrum antimicrobial activity by physicochemical interactions, ACS Appl. Nano Mater. 1 (2018) 3214–3225, https://doi.org/10.1021/acsanm.8b00402.

[12] L.Z. Flores-Lopez, H. Espinoza-Gomez, R. Somanathan, Silver nanoparticles: electron transfer, reactive oxygen species, oxidative stress, beneficial and toxicological effects. Mini review, J. Appl. Toxicol. 39 (2019) 16–26, https://doi.org/10.1002/jat.3654.

[13] A.A. Tayel, W.F. El-Tras, S. Moussa, A.F. El-Baz, H. Mahrous, M.F. Salem, L. Brimer, Antibacterial action of zinc oxide nanoparticles against foodborne pathogens, J. Food Saf. 31 (2011) 211–218, https://doi.org/10.1111/j.1745-4565.2010.00287.x.

[14] B. Khalandi, N. Asadi, M. Milani, S. Davaran, A.J.N. Abadi, E. Abasi, A. Akbarzadeh, A review on potential role of silver nanoparticles and possible mechanisms of their actions on bacteria, Drug Res. 67 (2017) 70–76, https://doi.org/10.1055/s-0042-113383.

[15] L. Yang, Z.P. Aguilar, F. Qu, H. Xu, H.Y. Xu, H. Wei, Enhanced antimicrobial activity of silver nanoparticles-Lonicera Japonica Thunb combo, IET Nanobiotechnol. 10 (2016) 28–32, https://doi.org/10.1049/iet-nbt.2015.0027.

[16] Y.A. Qing, L. Cheng, R.Y. Li, G.C. Liu, Y.B. Zhang, X.F. Tang, J.C. Wang, H. Liu, Y.G. Qin, Potential antibacterial mechanism of silver nanoparticles and the optimization of orthopedic implants by advanced modification technologies, Int. J. Nanomed. 13 (2018) 3311–3327, https://doi.org/10.2147/IJN.S165125.

[17] N. Wattanawong, K. Chatchaipaiboon, N. Sreekirin, D. Aht-ong, Migration, physical and antibacterial properties of silver zeolite/poly(butylene succinate) composite films for food packaging applications, J. Reinforc. Plast. Compos. 39 (2020) 95–110, https://doi.org/10.1177/0731684419893440.

[18] S.J. Chen, J. Popovich, N. Iannuzo, S.E. Haydel, D.K. Seo, Silver-ion-exchanged nanostructured zeolite X as antibacterial agent with superior ion release kinetics and efficacy against methicillin-resistant staphylococcus aureus, ACS Appl. Mater. Interfaces 9 (2017) 39271–39282, https://doi.org/10.1021/acsami.7b15001.

[19] A.A. Ahmed, A.A. Ali, A. El-Fiqi, Glass-forming compositions and physicochemical properties of degradable phosphate and silver-doped phosphate glasses in the P_2O_5-CaO-Na_2O-Ag_2O system, J. Mater. Res. Technol. 8 (2019) 1003–1013, https://doi.org/10.1016/j.jmrt.2018.07.012.

[20] Y. Koizumi, M. Taya, Kinetic evaluation of biocidal activity of titanium dioxide against phage MS2 considering interaction between the phage and photocatalyst particles, Biochem. Eng. J. 12 (2002) 107–116, https://doi.org/10.1016/S1369-703X(02)00046-3.

[21] P. Hajkova, P. Spatenka, J. Horsky, I. Horska, A. Kolouch, Photocatalytic effect of TiO_2 films on viruses and bacteria, Plasma Process. Polym. 4 (2007) S397–S401, https://doi.org/10.1002/ppap.200731007.

[22] O.L. Galkina, A. Sycheva, A. Blagodatskiy, G. Kaptay, V.L. Katanaev, G.A. Seisenbaeva, V.G. Kessler, A.V. Agafonov, The sol-gel synthesis of cotton/TiO_2 composites and their antibacterial properties, Surf. Coating. Technol. 253 (2014) 171–179, https://doi.org/10.1016/j.surfcoat.2014.05.033.

[23] M. Wang, Q.F. Zhao, H. Yang, D. Shi, J.C. Qian, Photocatalytic antibacterial properties of copper doped TiO_2 prepared by high-energy ball milling, Ceram. Int. 46 (2020) 16716–16724, https://doi.org/10.1016/j.ceramint.2020.03.246.

[24] M.I. Rahmah, Preparation of TiO_2/graphene nanostructure for antibacterial applications, Chem. Pap. 77 (2023) 3121–3128, https://doi.org/10.1007/s11696-023-02691-w.

[25] A.M. Awan, A. Khalid, P. Ahmad, A.I. Alharthi, M. Farooq, A. Khan, M.U. Khandaker, S. Aldawood, M.A. Alotaibi, A.A. El-Mansi, M.B. Eldesoqui, A.F. Dawood, S.H. Zyoud, Defects oriented hydrothermal synthesis of TiO_2 and $MnTiO_2$ nanoparticles as photocatalysts for wastewater treatment and antibacterial applications, Heliyon 10 (2024) e25579, https://doi.org/10.1016/j.heliyon.2024.e25579.

[26] Y. Rilda, D. Damara, Y.E. Putri, R. Refinel, A. Agustien, H. Pardi, Pseudomonas aeruginosa antibacterial textile cotton fiber construction based on ZnO-TiO_2 nanorods template, Heliyon 6 (2020) e03710, https://doi.org/10.1016/j.heliyon.2020.e03710.

[27] S. Abbad, K. Guergouri, S. Gazaout, S. Djebabra, A. Zertal, R. Barille, M. Zaabat, Effect of silver doping on the photocatalytic activity of TiO_2 nanopowders synthesized by the sol-gel route, J. Environ. Chem. Eng. 8 (2020) 103718, https://doi.org/10.1016/j.jece.2020.103718.

[28] M.A. Hossain, M. Elias, D.R. Sarker, Z.R. Diba, J.M. Mithun, M.A.K. Azad, I.A. Siddiquey, M.M. Rahman, J. Uddin, M.N. Uddin, Synthesis of Fe- or Ag-doped TiO_2-MWCNT nanocomposite thin films and their visible-light-induced catalysis of dye degradation and antibacterial activity, Res. Chem. Intermed. 44 (2018) 2667–2683, https://doi.org/10.1007/s11164-018-3253-z.
[29] Y. Jiang, X. Zhang, M.Y. Lu, C.Z. Bao, G.T. Liang, C.Z. Lai, W.Y. Shi, S.Y. Ma, Activity and characterization of Ce-Mo-Ti mixed oxide catalysts prepared by a homogeneous precipitation method for selective catalytic reduction of NO with NH_3, J. Taiwan Inst. Chem. Eng. 86 (2018) 78–89, https://doi.org/10.1016/j.jtice.2018.02.027.
[30] J.T. Xi, Y.P. Zhang, X. Chen, Y. Hu, A simple sol-gel hydrothermal method for the synthesis of defective TiO_2 nanocrystals with excellent visible-light photocatalytic activity, Res. Chem. Intermed. 46 (2020) 2205–2214, https://doi.org/10.1007/s11164-020-04087-x.
[31] R.J. Kamble, P.V. Gaikwad, K.M. Garadkar, S.R. Sabale, V.R. Puri, S.S. Mahajan, Photocatalytic degradation of malachite green using hydrothermally synthesized cobalt-doped TiO_2 nanoparticles, J. Iran. Chem. Soc. 19 (2022) 303–312, https://doi.org/10.1007/s13738-021-02303-y.
[32] K.N. Lin, J.L. Ma, X.P. Yang, D. N, Jin, Y.C. Li, G.J. Jiao, S.Q. Yao, S.L. Sun, R.C. Sun, Boosting electron kinetics of anatase TiO_2 with carbon nanosheet for efficient photo-reforming of xylose into biomass-derived organic acids, J. Alloys Compd. 906 (2022) 164276, https://doi.org/10.1016/j.jallcom.2022.164276.
[33] W.C. Cao, W.C. Wang, Z.X. Yang, W.H. Wang, W.G. Chen, K.C. Wu, Enhancing photocathodic protection performance by controlled synthesis of Bi/BiOBr/TiO_2 NTAs Z-scheme heterojunction films, J. Alloys Compd. 960 (2023) 170675, https://doi.org/10.1016/j.jallcom.2023.170675.
[34] J.P. Wang, P. Yang, B.B. Huang, Self-doped TiO_{2-x} nanowirs with enhanced photocatalytic activity: facile synthesis and effects of the Ti^{3+}, Appl. Surf. Sci. 356 (2015) 391–398, https://doi.org/10.1016/j.apsusc.2015.08.029.
[35] J.W. Li, Y.Y. Li, R. Chen, X. Zhu, D.D. Ye, Y. Yang, Y.X. Yu, D.C. Wang, Q. Liao, Solar energy storage by a microfluidic all-vanadium photoelectrochemical flow cell with self-doped TiO_2 photoanode, J. Energy Storage 43 (2021) 103228, https://doi.org/10.1016/j.est.2021.103228.
[36] R. Nawaz, S. Haider, H. Ullah, M.S. Akhtar, S. Khan, M. Junaid, N. Khan, Optimized remediation of treated agro-industrial effluent using visible light-responsive core-shell structured black TiO_2 photocatalyst, J. Environ. Chem. Eng. 10 (2022) 106968, https://doi.org/10.1016/j.jece.2021.106968.
[37] L. Wang, J. Ali, C.B. Zhang, G. Mailhot, G. Pan, Simultaneously enhanced photocatalytic and antibacterial activities of TiO_2/Ag composite nanofibers for wastewater purification, J. Environ. Chem. Eng. 8 (2020) 102104, https://doi.org/10.1016/j.jece.2017.12.057.
[38] G.H. Zhang, J.C. Wang, H.R. Zhang, T.Y. Zhang, S. Jiang, B. Li, H.L. Zhang, J.L. Cao, Facile synthesize hierarchical tubular micro-nano structured AgCl/Ag/TiO_2 hybrid with favorable visible light photocatalytic performance, J. Alloys Compd. 855 (2021) 157512, https://doi.org/10.1016/j.jallcom.2020.157512.
[39] H.C. Ma, W.B. Zheng, X. Yan, S.Z. Li, K. Zhang, G.J. Liu, L. Jiang, Polydopamine-induced fabrication of Ag-TiO_2 hollow nanospheres and their application in visible-light photocatalysis, Colloid. Surface. 586 (2020) 124283, https://doi.org/10.1016/j.colsurfa.2019.124283.
[40] F.B. Zeng, D.M. Luo, Z. Zhang, B. Liang, X.Z. Yuan, L. Fu, Study on the behavior of sulfur in hydrolysis process of titanyl sulfate solution, J. Alloys Compd. 670 (2016) 249–257, https://doi.org/10.1016/j.jallcom.2016.02.031.
[41] Y.F. Jiang, J.C. Hu, J.L. Li, Synthesis and visible light responsed photocatalytic activity of Sn doped Bi_2S_3 microspheres assembled by nanosheets, RSC Adv. 6 (2016) 39810–39817, https://doi.org/10.1039/C6RA02621D.
[42] B. Sun, G.W. Zhou, C.W. Shao, B. Jiang, J.L. Pang, Y. Zhang, Spherical mesoporous TiO_2 fabricated by sodium dodecyl sulfate-assisted hydrothermal treatment and its photocatalytic decomposition of papermaking wastewater, Powder Technol. 256 (2014) 118–125, https://doi.org/10.1016/j.powtec.2014.01.094.
[43] F. Tian, Y.P. Zhang, J. Zhang, C.X. Pan, Raman spectroscopy: a New approach to measure the percentage of anatase TiO_2 exposed (001) facets, J. Phys. Chem. C 116 (2012) 7515–7519, https://doi.org/10.1021/jp301256h.
[44] R. Ghamarpoor, A. Fallah, M. Jamshidi, Investigating the use of titanium dioxide (TiO_2) nanoparticles on the amount of protection against UV irradiation, Sci Rep-uk 13 (2023) 9793, https://doi.org/10.1038/s41598-023-37057-5.
[45] N. Moradi, M. Jamshidi, R. Ghamarpoor, M.R. Moghbeli, Surface functionalization/silane modification of CeO_2 nanoparticles and their influences on photocatalytic activity of acrylic films for methylene blue removal, Prog. Org. Coating 183 (2023) 107787, https://doi.org/10.1016/j.porgcoat.2023.107787.
[46] R. Ghamarpoor, A. Fallah, M. Jamshidi, S. Salehfekr, Using waste silver metal in synthesis of Z-scheme Ag@WO_3-CeO_2 heterojunction to increase photodegradation and electrochemical performances, J. Ind. Eng. Chem. 128 (2023) 459–471, https://doi.org/10.1016/j.jiec.2023.08.010.
[47] B.Z. Tian, R.F. Dong, J.M. Zhang, S.Y. Bao, F. Yang, J.L. Zhang, Sandwich-structured AgCl@Ag@TiO_2 with excellent visible-light photocatalytic activity for organic pollutant degradation and E. coli K12 inactivation, Appl. Catal. B Environ. 158–159 (2014) 76–84, https://doi.org/10.1016/j.apcatb.2014.04.008.
[48] F.L. Liang, Y. Yu, W. Zhou, X.Y. Xu, Z.H. Zhu, Highly defective CeO_2 as a promoter for efficient and stable water oxidation, J. Mater. Chem. A 3 (2015) 634–640, https://doi.org/10.1039/C4TA05770H.
[49] R. Ghamarpoor, M. Jamshidi, A. Fallah, F. Eftekharipour, Preparation of dual-use GPTES@ZnO photocatalyst from waste warm filter cake and evaluation of its synergic photocatalytic degradation for air-water purification, J. Environ. Manag. 342 (2023) 118352, https://doi.org/10.1016/j.jenvman.2023.118352.
[50] H. Ei-Hamshary, M.E. Ei-Naggar, T.A. Khattab, A. Ei-Faham, Preparation of multifunctional plasma cured cellulose fibers coated with photo-induced nanocomposite toward self-cleaning and antibacterial textiles, Polym. Bull. (Heidelberg, Ger.) 13 (2021) 3664, https://doi.org/10.3390/polym13213664.
[51] X.X. Xue, Y.Z. Wang, H. Yang, Preparation and characterization of boron-doped titania nano-materials with antibacterial activity, Appl. Surf. Sci. 264 (2013) 94–99, https://doi.org/10.1016/j.apsusc.2012.09.128.
[52] F. Eftekharipour, M. Jamshidi, R. Ghamarpoor, Fabricating core-shell of silane modified nano ZnO; Effects on photocatalytic degradation of benzene in air using acrylic nanocomposite, Alex. Eng. J. 70 (2023) 273–288, https://doi.org/10.1016/j.aej.2023.02.047.